The Oxidative Isomerisation of *cis,cis*-Dicarbonylmanganese(I) Derivatives; Isolation of the Resulting *trans*-Dicarbonylmanganese(II) Complexes and the *X*-Ray Structure of *cis,cis*-$[MnBr(CO)_2\{P(OPh)_3\}(Ph_2PCH_2PPh_2)]$ *

Neil G. Connelly, Keeley A. Hassard, Barry J. Dunne, A. Guy Orpen, and Stephen J. Raven
Department of Inorganic Chemistry, University of Bristol, Bristol BS8 1TS
Gabino A. Carriedo and Victor Riera
Department of Organometallic Chemistry, University of Oviedo, Oviedo 33071, Spain

The manganese(I) complexes *cis,cis*-$[MnL(CO)_2\{P(OPh)_3\}(dppm)]^z$ [**1**; $z = 0$, L = Br, NCS, or CN; $z = +1$, L = pyridine (py), NCMe, CNMe, or $P(OPh)_3$; dppm = $Ph_2PCH_2PPh_2$], *cis,cis*-$[Mn(CO)_2LL'(dppe)]^+$ [L = $P(OPh)_3$, L′ = py or NCMe; L = L′ = $P(OEt)_3$; dppe = $Ph_2PCH_2CH_2PPh_2$], and *cis*-$[Mn(CO)_2(dppm)_2]^+$ undergo oxidative isomerisation at a platinum electrode in CH_2Cl_2 to the *trans*-dicarbonylmanganese(II) analogues which are also formed directly by the reversible one-electron oxidation of *trans*-$[MnL(CO)_2\{P(OPh)_3\}(dppm)]^z$ (**2**; $z = 0$, L = Br or CN; $z = +1$, L = CNMe) or *trans*-$[Mn(CO)_2\{P(OEt)_3\}_2(dppe)]^+$. The low-spin manganese(II) complexes *trans*-$[MnL(CO)_2\{P(OPh)_3\}(dppm)]^z$ (**3**; $z = +1$, L = Br or CN) have been prepared as crystalline $[PF_6]^-$ salts by the chemical oxidation of (**1**; $z = 0$, L = Br or CN) with $[NO][PF_6]$ and $[N(C_6H_4Br\text{-}p)_3][PF_6]$ respectively, but excess $[NO][PF_6]$ and (**1**; $z = 0$, L = CN) gave the hydrogen isocyanide complex (**3**; $z = +2$, L = CNH); the e.s.r. spectra of these species are reported. The stereochemistry of *cis,cis*-$[MnBr(CO)_2\{P(OPh)_3\}(dppm)]$ has been determined by *X*-ray crystallography. The bromide ligand is *trans* to CO, and the manganese has a distorted octahedral co-ordination geometry with the largest distortions due to the restricted bite of the chelating dppm ligand [P–Mn–P 71.4(1)°]. The structure analysis has aided a brief discussion of the significance of the linear correlations between E^0 and the ligand constant, P_L, observed for both (**1**) and (**2**).

The oxidative isomerisation reactions of phosphine derivatives of $[MnBr(CO)_5]$ and $[Mn(CO)_6]^+$ have been studied by both electrochemical [1–4] and chemical [1–3,5–8] methods. The former have led to the partial quantification of the kinetics and thermodynamics associated with the process, and the latter have largely been used to provide synthetic routes to otherwise inaccessible isomers.[5–7] In all of these studies, the manganese(II) oxidation products have been only partially characterised at best.

As part of a wider study of the redox properties of mono-[9–11] and poly-nuclear [12] manganese carbonyl complexes, we recently reported[9] on the reversible one-electron oxidation of *trans*-$[MnL(CO)(dppm)_2]^z$ ($z = 0$, L = Br, NCS, or CN; $z = +1$, L = NCMe, CNMe, CNBu^t, or CO; dppm = $Ph_2PCH_2PPh_2$) and in particular on the preparation of the paramagnetic salts *trans*-$[MnL(CO)(dppm)_2][PF_6]_2$ (L = CNMe or CNBu^t). We now describe chemical and electrochemical studies of the oxidative isomerisation of *cis,cis*-$[MnL(CO)_2\{P(OPh)_3\}(dppm)]^z$ and the isolation and full characterisation of the products, namely *trans*-$[MnL(CO)_2\{P(OPh)_3\}(dppm)]^{z+1}$. In addition, the structure of *cis,cis*-$[MnBr(CO)_2\{P(OPh)_3\}(dppm)]$ has been fully defined by *X*-ray crystallography, allowing discussion of the significance of the observed linear correlations between the oxidation potential, E^0, and ligand constant, P_L,[13] for both *cis,cis*- and *trans*-$[MnL(CO)_2\{P(OPh)_3\}(dppm)]$.

Results and Discussion

Electrochemical Studies.—The cyclic voltammograms of *cis,cis*-$[MnL(CO)_2\{P(OPh)_3\}(dppm)]^z$ [**1**; $z = 0$, L = Br, NCS, or CN; $z = +1$, L = pyridine (py), NCMe, CNMe, or $P(OPh)_3$], *cis,cis*-$[Mn(CO)_2LL'(dppe)]^+$ [L = $P(OPh)_3$, L′ = py or NCMe; L = L′ = $P(OEt)_3$; dppe = $Ph_2PCH_2CH_2PPh_2$], and *cis*-$[Mn(CO)_2(dppm)_2]^+$, in CH_2Cl_2 at platinum, are qualitatively similar; each shows a diffusion controlled ($i_{ox}/\sqrt{v}$ constant for scan rates $50 \leqslant v \leqslant 500$ mV s^{-1}) oxidation wave in the potential range 0.8—1.8 V with an associated product wave at a more negative potential. The reversibility of the first process varies considerably such that (**1**; $z = 0$, L = NCS) shows a fully reversible wave ($i_{red}/i_{ox} = 1.01$) at a scan rate of 500 mV s^{-1} whereas (**1**; $z = 0$, L = CN; $z = +1$, L = py) and *cis,cis*-$[Mn(CO)_2(py)\{P(OPh)_3\}(dppm)]^+$ show totally irreversible behaviour even at 1 V s^{-1}. In most cases, the oxidation is partially reversible at 200 mV s^{-1} so that an estimate of E^0, taken as equal to $[(E_p)_{ox} + (E_p)_{red}]/2$ [$(E_p)_{ox}$ = oxidation peak potential, $(E_p)_{red}$ = reduction peak potential], can be made (Table 1). For (**1**; $z = 0$, L = CN; $z = +1$, L = py) the $(E_p)_{ox}$ values at 200 mV s^{-1} are tabulated.

The cyclic voltammetry of (**1**; $z = 0$, L = Br) is representative of most of the complexes in Table 1 and is illustrated in Figure 1. The first scan [Figure 1(*a*)] shows the partially reversible oxidation wave at *ca.* 0.9 V and the associated product wave at *ca.* 0.27 V; the second and subsequent scans [Figure 1(*b*)] reveal that the product reduction peak is part of a reversible wave centred at 0.31 V.

That the oxidation of (**1**), and the other *cis,cis* complexes noted above, results in isomerisation and the formation of *trans*-dicarbonylmanganese(II) complexes is readily demonstrated by cyclic voltammetric studies on *trans*-$[MnL(CO)_2\{P(OPh)_3\}(dppm)]^z$ (**2**; $z = 0$, L = Br or CN; $z = +1$, L = CNMe). Each of these species shows one fully reversible, diffusion-controlled oxidation wave at a potential (Table 1) identical to that of the product formed by oxidising (**1**; $z = 0$, L = Br or CN; $z = 1$, L = CNMe).

The controlled potential oxidation of (**1**) also provides

---

* *cis,cis*-[Bis(diphenylphosphino)methane]bromodicarbonyl(triphenyl phosphite)manganese(I).

Supplementary data available: see Instructions for Authors, *J. Chem. Soc., Dalton Trans.*, 1988, Issue 1, pp. xvii—xx.

Table 1. Cyclic voltammetric data[a] for dicarbonylmanganese(I) complexes

Complex	E^0/V		L	P_L/V[c]
	trans	*cis,cis*[b]		
$[MnBr(CO)_2\{P(OPh)_3\}(dppm)]$	0.31	0.86	Br	−1.17
$[Mn(NCS)(CO)_2\{P(OPh)_3\}(dppm)]$	0.47[d]	0.93	NCS	−1.03[e]
$[Mn(CN)(CO)_2\{P(OPh)_3\}(dppm)]$	0.64	1.12[f]	CN	−1.00
$[Mn(CO)_2(py)\{P(OPh)_3\}(dppm)][PF_6]$	0.93[d]	1.43[f]	py	−0.59
$[Mn(CO)_2(NCMe)\{P(OPh)_3\}(dppm)][PF_6]$	1.05[d]	1.46	NCMe	−0.58
$[Mn(CO)_2(CNMe)\{P(OPh)_3\}(dppm)][PF_6]$	1.29	1.57	CNMe	−0.43
$[Mn(CO)_2\{P(OPh)_3\}_2(dppm)][PF_6]$	1.39[d]	1.67	$P(OPh)_3$	−0.18
$[Mn(CO)_2(py)\{P(OPh)_3\}(dppe)][PF_6]$	0.97[d]	1.44[f]	—	—
$[Mn(CO)_2(NCMe)\{P(OPh)_3\}(dppe)][PF_6]$	1.01[d]	1.46	—	—
$[Mn(CO)_2\{P(OEt)_3\}_2(dppe)][PF_6]$	1.09	1.38	—	—
$[Mn(CO)_2(dppm)_2][PF_6]$	0.88[d]	1.30	—	—

[a] Potentials are *versus* the aqueous saturated calomel electrode, measured at a platinum bead in CH_2Cl_2 with 0.1 mol dm^{-3} $[NBu^n{}_4][PF_6]$ as supporting electrolyte. Under these conditions, the E^0 values for the complexes $[Fe(\eta\text{-}C_5H_5)_2]^+$–$[Fe(\eta\text{-}C_5H_5)_2]$ and $[Fe(\eta\text{-}C_5Me_5)_2]^+$–$[Fe(\eta\text{-}C_5Me_5)_2]$ are 0.47 and −0.07 V respectively. [b] Unless otherwise stated, the potential given is equal to $[(E_p)_{ox} + (E_p)_{red}]/2$ and is measured from cyclic voltammograms taken at sufficiently high scan rates for the oxidation of the *cis,cis* isomer to show at least partial reversibility. [c] Ligand constants for ligand L, taken from ref. 13 unless stated otherwise. [d] Data taken from the cyclic voltammogram of the *cis,cis* isomer (see text). [e] From ref. 9. [f] Completely irreversible wave; the potential given is $(E_p)_{ox}$ at a scan rate of 200 mV s^{-1}.

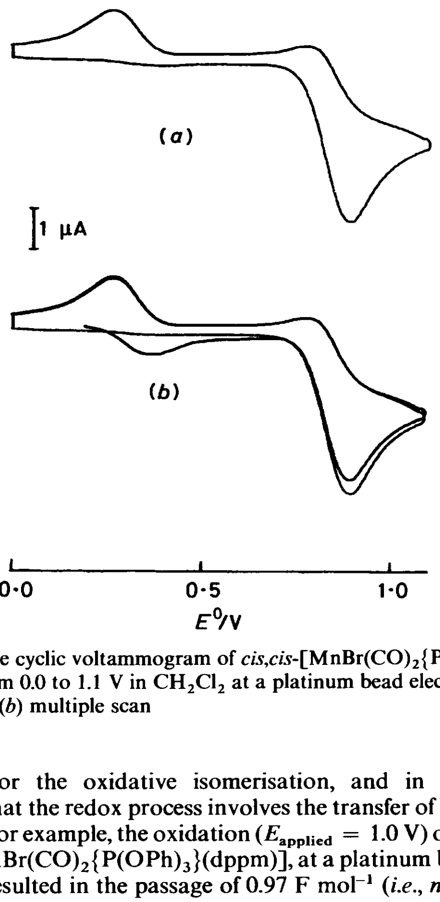

Figure 1. The cyclic voltammogram of *cis,cis*-$[MnBr(CO)_2\{P(OPh)_3\}(dppm)]$ from 0.0 to 1.1 V in CH_2Cl_2 at a platinum bead electrode: (*a*) single scan, (*b*) multiple scan

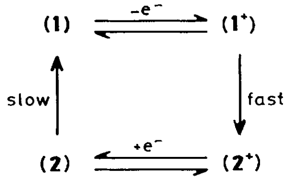

Figure 2. The 'square-scheme' for the oxidative isomerisation of *cis,cis*-$[MnL(CO)_2\{P(OPh)_3\}(dppm)]^z$ (**1**) to *trans*-$[MnL(CO)_2\{P(OPh)_3\}(dppm)]^z$ (**2**)

evidence for the oxidative isomerisation, and in addition confirms that the redox process involves the transfer of only one electron. For example, the oxidation ($E_{applied}$ = 1.0 V) of orange *cis,cis*-$[MnBr(CO)_2\{P(OPh)_3\}(dppm)]$, at a platinum basket in CH_2Cl_2, resulted in the passage of 0.97 F mol^{-1} (*i.e.*, n = 0.97) and the formation of a dark red solution showing one *reduction* wave (cyclic and rotating platinum electrode voltammetry) at a potential (0.31 V) identical to that for the oxidation of (**2**; z = 0, L = Br).

The oxidation of (**1**) can be described by the 'square-scheme' shown in Figure 2, as proposed[1–3] to account for the electrochemical behaviour of *fac*- and *mer*-$[MX(CO)_3L_2]$ [M = Mn or Re, X = Cl or Br, L_2 = dppm, dppe, *etc.*; L = PPh_3, $P(OPh)_3$, $SbPh_3$, *etc.*]. The kinetics and thermodynamics associated with the oxidative isomerisation of *fac*-$[MnCl(CO)_3(dppm)]$ have been partially quantified, with the *fac* cation converting to the *mer* isomer *via* a non-dissociative twist mechanism. We have not quantified the processes involved for the conversion of (**1**) to (**2**), but the observed variation in the reversibility of the oxidation wave for (**1**) with the ligand L (see above) suggests qualitatively that the rate of isomerisation, k_{iso}, of (1^+) to (2^+) increases in the order L = CN, py > Br, CNMe, NCMe, $P(OPh)_3$ > NCS.

The data* given in Table 1 show that E^0 [or $(E_p)_{ox}$ for those complexes which are irreversibly oxidised] for the oxidation of (**1**) and (**2**) depends in the expected way on the overall charge of the complex, z, and on the donor–acceptor abilities of the ligand, L. For the two cases where comparison is possible (Table 1), the effect on E^0 of replacing dppm, in (**1**) or (**2**), by dppe is minimal. A similar independence of the chelating ligand was also observed[14] for *cis*-$[M(CO)_2(L\text{–}L)_2]$ (M = Mo or W, L–L = dppm or dppe) but there is a surprisingly large effect in the *trans* isomers in that the dppm complexes are more readily oxidised by *ca.* 0.2—0.3 V.

The potential data in Table 1 may be further analysed if considered in conjunction with the ligand constant P_L as defined by Chatt *et al.*[13] [equation (1)].

$$P_L = E^0[Cr(CO)_5L] - E^0[Cr(CO)_6] \qquad (1)$$

---

* In some cases, the *trans* isomer (**2**) was not studied directly by cyclic voltammetry; the E^0 value for the couple (**2**)–(2^+) was measured from the product wave in the cyclic voltammogram of the appropriate *cis,cis* isomer (**1**).

Table 2. Bond lengths (Å) for *cis,cis*-[$MnBr(CO)_2\{P(OPh)_3\}(dppm)$]

Mn(1)–Br(1)	2.527(1)	Mn(1)–C(8)	1.792(6)
Mn(1)–C(9)	1.778(6)	Mn(1)–P(1)	2.217(2)
Mn(1)–P(2)	2.302(2)	Mn(1)–P(3)	2.362(2)
C(8)–O(8)	1.173(7)	C(9)–O(9)	1.138(7)
P(1)–O(1)	1.609(4)	P(1)–O(2)	1.598(4)
P(1)–O(3)	1.620(4)	O(1)–C(11)	1.406(7)
C(11)–C(12)	1.343(9)	C(11)–C(16)	1.375(9)
C(12)–C(13)	1.398(10)	C(13)–C(14)	1.362(11)
C(14)–C(15)	1.348(11)	C(15)–C(16)	1.394(9)
O(2)–C(21)	1.393(7)	C(21)–C(22)	1.384(8)
C(21)–C(26)	1.368(9)	C(22)–C(23)	1.384(11)
C(23)–C(24)	1.387(12)	C(24)–C(25)	1.371(12)
C(25)–C(26)	1.395(9)	O(3)–C(31)	1.416(6)
C(31)–C(32)	1.362(10)	C(31)–C(36)	1.372(10)
C(32)–C(33)	1.411(12)	C(33)–C(34)	1.368(21)
C(34)–C(35)	1.372(16)	C(35)–C(36)	1.394(12)
C(10)–P(2)	1.836(5)	C(10)–P(3)	1.839(5)
P(2)–C(41)	1.819(6)	P(2)–C(51)	1.824(5)
C(41)–C(42)	1.380(8)	C(41)–C(46)	1.380(8)
C(42)–C(43)	1.368(10)	C(43)–C(44)	1.377(10)
C(44)–C(45)	1.360(10)	C(45)–C(46)	1.406(10)
C(51)–C(52)	1.373(8)	C(51)–C(56)	1.371(8)
C(52)–C(53)	1.392(9)	C(53)–C(54)	1.365(10)
C(54)–C(55)	1.351(11)	C(55)–C(56)	1.376(9)
P(3)–C(61)	1.826(6)	P(3)–C(71)	1.830(6)
C(61)–C(62)	1.367(8)	C(61)–C(66)	1.400(8)
C(62)–C(63)	1.403(12)	C(63)–C(64)	1.365(15)
C(64)–C(65)	1.324(14)	C(65)–C(66)	1.394(12)
C(71)–C(72)	1.383(9)	C(71)–C(76)	1.392(8)
C(72)–C(73)	1.383(10)	C(73)–C(74)	1.351(12)
C(74)–C(75)	1.386(14)	C(75)–C(76)	1.382(9)

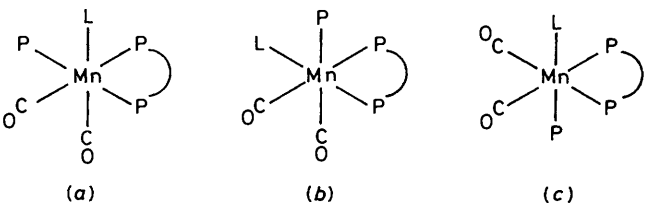

(*a*) (*b*) (*c*)

Figure 3. Three possible structures for (**1**); P = $P(OPh)_3$, P–P = $Ph_2PCH_2PPh_2$

For several series of octahedral metal complexes, such as *trans*-[$MoL(CO)(dppe)_2$], [$ReL(N_2)(dppe)_2$]$^+$, *etc*., linear correlations between E^0 and P_L were found and were described by equation (2) where E_s and β were taken as measures of the

$$E^0 = E_s + \beta \cdot P_L \qquad (2)$$

electron-richness and polarisability respectively of the square-pyramidal binding site to which the ligand L is bound.[13]

For complexes (**1**) and (**2**) the plots of E^0 *vs.* P_L are also linear (correlation coefficients of 0.983 and 0.982 respectively) and E_s and β values of 1.90 V and 0.88, and 1.66 V and 1.11 respectively can be calculated.*

Table 3. Bond angles (°) for *cis,cis*-[$MnBr(CO)_2\{P(OPh)_3\}(dppm)$]

Br(1)–Mn(1)–C(8)	89.1(2)	Br(1)–Mn(1)–C(9)	175.9(2)
C(8)–Mn(1)–C(9)	87.0(3)	Br(1)–Mn(1)–P(1)	90.6(1)
C(8)–Mn(1)–P(1)	97.3(2)	C(9)–Mn(1)–P(1)	90.9(2)
Br(1)–Mn(1)–P(2)	88.2(1)	C(8)–Mn(1)–P(2)	95.8(2)
C(9)–Mn(1)–P(2)	91.2(2)	P(1)–Mn(1)–P(2)	166.8(1)
Br(1)–Mn(1)–P(3)	87.4(1)	C(8)–Mn(1)–P(3)	166.9(2)
C(9)–Mn(1)–P(3)	96.2(2)	P(1)–Mn(1)–P(3)	95.4(1)
P(2)–Mn(1)–P(3)	71.4(1)	Mn(1)–C(8)–O(8)	176.7(5)
Mn(1)–C(9)–O(9)	176.5(5)	Mn(1)–P(1)–O(1)	110.3(2)
Mn(1)–P(1)–O(2)	118.5(1)	O(1)–P(1)–O(2)	100.2(2)
Mn(1)–P(1)–O(3)	122.4(1)	O(1)–P(1)–O(3)	104.0(2)
O(2)–P(1)–O(3)	98.4(2)	P(1)–O(1)–C(11)	130.5(4)
O(1)–C(11)–C(12)	115.7(5)	O(1)–C(11)–C(16)	123.6(5)
C(12)–C(11)–C(16)	120.7(6)	C(11)–C(12)–C(13)	120.2(7)
C(12)–C(13)–C(14)	119.1(7)	C(13)–C(14)–C(15)	120.9(7)
C(14)–C(15)–C(16)	120.2(7)	C(11)–C(16)–C(15)	118.8(6)
P(1)–O(2)–C(21)	133.3(3)	O(2)–C(21)–C(22)	116.8(5)
O(2)–C(21)–C(26)	122.3(5)	C(22)–C(21)–C(26)	120.8(6)
C(21)–C(22)–C(23)	119.2(6)	C(22)–C(23)–C(24)	120.5(7)
C(23)–C(24)–C(25)	119.6(7)	C(24)–C(25)–C(26)	120.3(7)
C(21)–C(26)–C(25)	119.6(6)	P(1)–O(3)–C(31)	120.7(3)
O(3)–C(31)–C(32)	117.6(6)	O(3)–C(31)–C(36)	119.8(5)
C(32)–C(31)–C(36)	122.4(6)	C(31)–C(32)–C(33)	119.1(9)
C(32)–C(33)–C(34)	118.0(10)	C(33)–C(34)–C(35)	122.8(10)
C(34)–C(35)–C(36)	118.8(10)	C(31)–C(36)–C(35)	118.8(7)
P(2)–C(10)–P(3)	95.6(3)	Mn(1)–P(2)–C(10)	95.3(2)
Mn(1)–P(2)–C(41)	114.3(2)	C(10)–P(2)–C(41)	108.2(3)
Mn(1)–P(2)–C(51)	129.2(2)	C(10)–P(2)–C(51)	105.6(2)
C(41)–P(2)–C(51)	102.4(2)	P(2)–C(41)–C(42)	117.5(4)
P(2)–C(41)–C(46)	124.4(4)	C(42)–C(41)–C(46)	117.9(6)
C(41)–C(42)–C(43)	121.7(6)	C(42)–C(43)–C(44)	120.4(6)
C(43)–C(44)–C(45)	119.5(7)	C(44)–C(45)–C(46)	120.1(6)
C(41)–C(46)–C(45)	120.5(6)	P(2)–C(51)–C(52)	121.8(4)
P(2)–C(51)–C(56)	119.7(4)	C(52)–C(51)–C(56)	118.5(5)
C(51)–C(52)–C(53)	119.7(6)	C(52)–C(53)–C(54)	120.6(6)
C(53)–C(54)–C(55)	119.5(6)	C(54)–C(55)–C(56)	120.3(7)
C(51)–C(56)–C(55)	121.2(6)	Mn(1)–P(3)–C(10)	93.3(2)
Mn(1)–P(3)–C(61)	120.0(2)	C(10)–P(3)–C(61)	104.6(3)
Mn(1)–P(3)–C(71)	127.1(2)	C(10)–P(3)–C(71)	106.7(3)
C(61)–P(3)–C(71)	101.9(3)	P(3)–C(61)–C(62)	121.1(5)
P(3)–C(61)–C(66)	119.9(4)	C(62)–C(61)–C(66)	118.9(6)
C(61)–C(62)–C(63)	120.1(7)	C(62)–C(63)–C(64)	119.5(8)
C(63)–C(64)–C(65)	121.1(10)	C(64)–C(65)–C(66)	121.0(8)
C(61)–C(66)–C(65)	119.2(6)	P(3)–C(71)–C(72)	120.1(5)
P(3)–C(71)–C(76)	121.4(5)	C(72)–C(71)–C(76)	118.4(5)
C(71)–C(72)–C(73)	120.7(6)	C(72)–C(73)–C(74)	120.8(7)
C(73)–C(74)–C(75)	119.7(7)	C(74)–C(75)–C(76)	120.3(7)
C(71)–C(76)–C(75)	120.1(6)		

In order to discuss the significance of these E_s and β values it is necessary to know the structures of the $Mn(CO)_2\{P(OPh)_3\}(dppm)$ binding sites in (**1**) and (**2**). There is only one possible structure for the *trans* complexes (**2**), but there are three for the *cis,cis* species (**1**) as shown in Figure 3. On the basis of chemical studies[5] and ^{31}P n.m.r. spectroscopy,[15] the structure shown in Figure 3(*a*) has been proposed, but in order to remove any possible ambiguity the *X*-ray crystal structure of *cis,cis*-[$MnBr(CO)_2\{P(OPh)_3\}(dppm)$] was determined.

The molecular structure of (**1**; z = 0, L = Br) is illustrated in Figure 4; Tables 2 and 3 list the derived bond lengths and interbond angles respectively and Table 4 the atomic co-ordinates. The isomer is clearly of the type shown in Figure 3(*a*) with bromine *trans* to CO. The largest angular distortions from regular octahedral geometry about Mn(1) are due to the small bite of the chelating dppm ligand [P(2)–Mn(1)–P(3) 71.4(1)°]. The 18.6° reduction of this angle from the ideal 90° is shared approximately equally between the other *cis* angles in the Mn(1)P(1)P(2)P(3)C(8) plane, which range from 95.4(1) to

---

* For these plots, P_L(NCS) has been taken as −1.03 V (for reasons given in ref. 9) rather than −0.88 V as calculated by Chatt *et al.*,[13] and the E^0 values of (**1**; z = 0, L = CN, E^0 = 1.07 V; **1**; z = 1, L = py, E^0 = 1.38 V) have been estimated. The peak separation, $(E_p)_{ox}-(E_p)_{red}$ for the oxidations of (**1**), (**2**), and [$Fe(\eta\text{-}C_5H_5)_2$], at a cyclic voltammetric scan rate of 200 mV s^{-1}, are *ca.* 100 mV under the experimental conditions used. Thus, the E^0 values of the cyanide and pyridine complexes, which are irreversibly oxidised (see above), were estimated from $E^0 = (E_p)_{ox} - 50$ mV.

Table 4. Atomic co-ordinates (× 10^4) for *cis,cis*-[$MnBr(CO)_2\{P(OPh)_3\}$(dppm)]

Atom	*x*	*y*	*z*	Atom	*x*	*y*	*z*
Mn(1)	2 465(1)	−249(1)	1 373(1)	C(10)	1 313(4)	294(3)	496(2)
Br(1)	1 056(1)	141(1)	1 734(1)	P(2)	2 280(1)	664(1)	859(1)
C(8)	3 137(4)	203(3)	1 828(2)	C(41)	3 204(4)	779(3)	486(2)
O(8)	3 586(3)	523(2)	2 110(2)	C(42)	400 4(4)	1 047(3)	693(2)
C(9)	3 501(4)	−479(3)	1 143(2)	C(43)	4 761(5)	1 095(4)	452(3)
O(9)	4 186(3)	−613(2)	1 017(1)	C(44)	4 740(5)	876(3)	−10(3)
P(1)	2 423(1)	−1 245(1)	1 745(1)	C(45)	3 955(5)	625(3)	−229(2)
O(1)	3 364(3)	−1 648(2)	1 720(1)	C(46)	3 182(4)	566(3)	21(2)
C(11)	3 593(4)	−2 333(3)	1 827(2)	C(51)	1 956(4)	1 544(3)	977(2)
C(12)	4 298(4)	−2 584(3)	1 616(3)	C(52)	2 090(4)	1 825(3)	1 421(2)
C(13)	4 598(5)	−3 253(4)	1 709(3)	C(53)	1 862(5)	2 507(3)	1 491(3)
C(14)	4 167(5)	−3 644(4)	2 017(3)	C(54)	1 457(5)	2 887(3)	1 128(3)
C(15)	3 450(5)	−3 397(3)	2 224(3)	C(55)	1 310(6)	2 606(4)	693(3)
C(16)	3 163(5)	−2 725(3)	2 141(2)	C(56)	1 546(5)	1 936(3)	618(2)
O(2)	1 727(3)	−1 815(2)	1 533(1)	P(3)	1 510(1)	−591(1)	703(1)
C(21)	965(4)	−2 118(3)	1 698(2)	C(61)	1 988(4)	−1 022(3)	211(2)
C(22)	936(5)	−2 827(3)	1 699(2)	C(62)	1 614(6)	−944(4)	−244(2)
C(23)	171(6)	−3 154(4)	1 833(2)	C(63)	1 991(7)	−1 282(5)	−616(3)
C(24)	−565(5)	−2 777(4)	1 957(3)	C(64)	2 717(8)	−1 705(5)	−519(4)
C(25)	−525(4)	−2 076(4)	1 954(2)	C(65)	3 079(6)	−1 796(4)	−79(4)
C(26)	250(4)	−1 742(3)	1 829(2)	C(66)	2 725(4)	−1 467(3)	300(2)
O(3)	2 223(2)	−1 302(3)	2 296(1)	C(71)	397(4)	−997(3)	698(2)
C(31)	2 707(5)	−893(3)	2 644(2)	C(72)	289(4)	−1 678(3)	572(2)
C(32)	2 225(6)	−439(4)	2 886(2)	C(73)	−533(5)	−2 004(4)	598(2)
C(33)	2 684(10)	−31(5)	3 242(3)	C(74)	−1 255(5)	−1 660(5)	736(3)
C(34)	3 598(11)	−120(5)	3 333(4)	C(75)	−1 166(4)	−976(5)	863(2)
C(35)	4 078(7)	−593(5)	3 099(3)	C(76)	−345(4)	−645(3)	844(2)
C(36)	3 621(5)	−988(4)	2 745(2)				

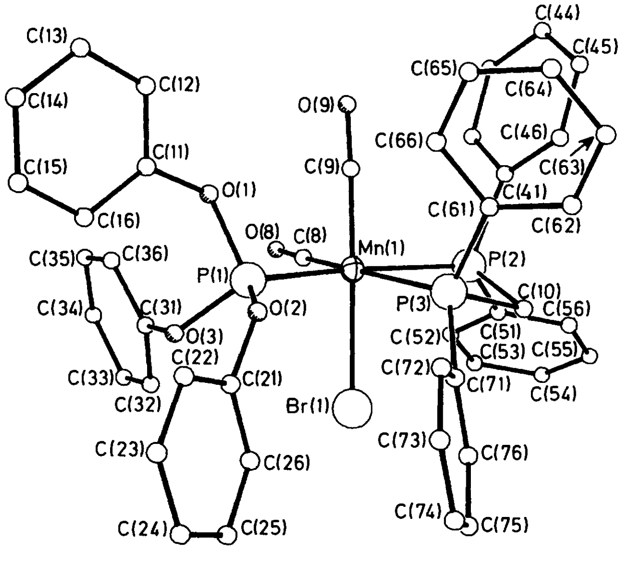

Figure 4. Molecular structure of *cis,cis*-[$MnBr(CO)_2\{P(OPh)_3\}$(dppm)] (**1**; z = 0, L = Br) showing the atomic labelling scheme. All hydrogen atoms have been omitted for clarity

97.3(2)°. The four-membered ring formed by the dppm ligand is rather puckered [hence intraring torsion angles ≠ 0, *e.g.* Mn(1)–P(2)–C(10)–P(3) −17.7°] thereby relieving some steric hindrance due to eclipsing of ring bonds at the expense of some diminution of bond angles in the ring [*e.g.* P(2)–C(10)–P(3) 95.6(3), Mn(1)–P(2)–C(10) 95.3(2), and Mn(1)–P(3)–C(10) 93.3(2)°].

The Mn–CO distances show insignificant variation despite having differing *trans* ligands [Mn(1)–C(9) 1.778(6) *vs.* Mn(1)–C(8) 1.792(6) Å]. The Mn–P distances are dependent both on the substituents at phosphorus and on the *trans* ligand, as would be expected; thus Mn(1)–P(1) is the shortest [2.217(2) Å], Mn(1)–P(2) [*trans* to P(1)] the next [2.302(2) Å], and Mn(1)–P(3) the longest [*trans* to CO, 2.362(2) Å]. Other aspects of the molecular and crystal structure are not unusual.

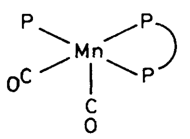

(I)

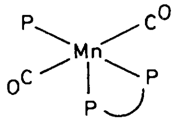

(II)

P = $P(OPh)_3$ P—P = $Ph_2PCH_2PPh_2$

The *X*-ray study of (**1**; L = Br), taken with the electrochemical results for (**1**) and (**2**), now show that limitations must be placed on the use of equation (2). According to this equation, the E^0 value for an octahedral complex [$M(CO)L_n$] is also the E_s value for the binding site ML_n [this follows from equation (1) which defines P_L(CO) = 0.0 V]. Thus, the E_s values for the binding sites (**I**) and (**II**) should be equal, the addition of CO to either site giving the same complex, namely *mer*-[$Mn(CO)_3\{P(OPh)_3\}$(dppm)]$^+$. However the calculated values of E_s for (**I**) and (**II**) differ by 0.24 V (see above) a difference which cannot result from experimental error.

We conclude, therefore, that equation (2) is useful for comparative purposes in strictly limited cases only. For structurally similar sites such as [$Mn(CO)(dppm)_2$]$^+$,[9] [$MoX(dppe)_2$]^z (z = +1, X = NO; z = 0, X = CO, N_2, or NCPh; z = −1, X = N_3),[13] [$FeH(dppe)_2$]$^+$,[13] and [$Re(N_2)(dppe)_2$]$^+$,[13] all of which have two chelating bis(phosphine) ligands in the equatorial positions, the use of equation (2) leads to a meaningful comparison of the effects of the axial ligand, metal, and charge on the binding site

Table 5. I.r. spectroscopic and analytical data for *trans*-$[MnL(CO)_2\{P(OPh)_3\}(dppm)]^z$ (**3**)

L	z	$\tilde{\nu}(CO)^a/cm^{-1}$	Analysis[b] (%) C	H	N
Br	+1	1 993	52.5 (52.4)	3.7 (3.6)	—
CN	+1	2 002	56.3 (56.6)	4.1 (3.8)	1.4 (1.4)
CNH	+2	2 008[c]	49.4 (49.3)	3.4 (3.4)	1.5 (1.3)

[a] In CH_2Cl_2. [b] Analysis for $[PF_6]^-$ salts; calculated values in parentheses. [c] $\tilde{\nu}(CN)$ at 2 142 cm^{-1}.

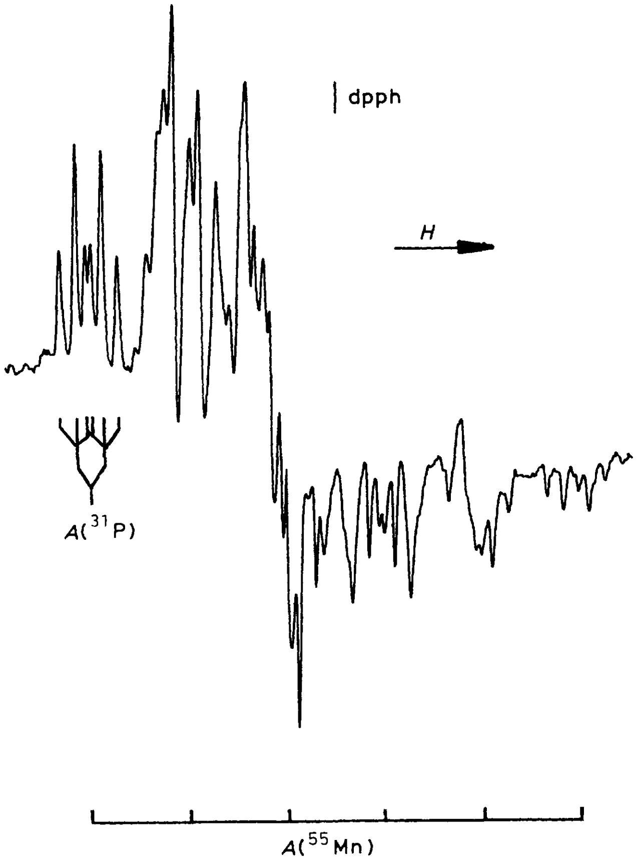

Figure 5. The e.s.r. spectrum of *trans*-$[Mn(CN)(CO)_2\{P(OPh)_3\}(dppm)]^+$ in a CH_2Cl_2–thf glass at −110 °C

properties. However, the equation cannot be used to make comparison between isomeric binding sites such as (**I**) and (**II**). It is clear that in general the particular interaction of a given ligand, L, with the orbitals of a site, M_s, in a complex, M_sL, will depend on the geometry of M_s (nature of *cis* and *trans* ligands, *etc.*) and not be solely determined by the composition of the complex. Equation (2) makes no provision for this dependence, despite its utility in describing the variation of E_s with L at a given site.

The Chemical Oxidation of (**1**) *and* (**2**).—The electrochemical data given in Table 1 suggest that at least for the neutral complexes of the series (L = Br, NCS, or CN) chemical oxidation of (**1**) or (**2**) should provide a route to the dicarbonylmanganese(II) complexes *trans*-$[MnL(CO)_2\{P(OPh)_3\}(dppm)]^z$ (**3**). In addition, the electrolytic study on (**1**; z = 0, L = Br) implied that (**3**; z = +1, L = Br) should be stable on the preparative timescale.

The addition of $[NO][PF_6]$ to (**1**; z = 0, L = Br) in CH_2Cl_2 gave an intense crimson solution from which analytically pure crimson crystals were readily isolated in good yield. The crystals show one carbonyl band in the i.r. spectrum (Table 5) *ca.* 70 cm^{-1} to higher wavenumber than that of (**2**; z = 0, L = Br), in agreement with the formulation of the complex as *trans*-$[MnL(CO)_2\{P(OPh)_3\}(dppm)]^z$ (**3**; L = Br, z = +1); the cyclic and rotating platinum electrode voltammograms confirm this formulation, showing one fully reversible reduction wave at a potential identical to that for the oxidation of (**2**; z = 0, L = Br).

The chemical oxidation of (**2**; z = 0, L = CN) is somewhat more complex than that of (**2**; z = 0, L = Br). Using a stoicheiometric (1:1) quantity of $[N(C_6H_4Br\text{-}p)_3][PF_6]$ as oxidant, crimson crystals of the $[PF_6]^-$ salt of (**3**; z = +1, L = CN) were isolated and characterised as above (Table 5). However, the addition of an excess of $[NO][PF_6]$ to the *cis,cis*-cyanide complex in CH_2Cl_2 resulted first in the formation of a crimson solution of (**3**; z = +1, L = CN) and then in a purple solution from which purple crystals of the hydrogen isocyanide complex (**3**; z = 2, L = CNH) were isolated; the HNC ligand most probably results from protonation of (**3**; z = +1, L = CN) by HPF_6, formed from excess $[NO][PF_6]$ and traces of water in the solvent.

The cyclic voltammogram of (**3**; z = +1, L = CN) is similar to that of (**3**; z = +1, L = Br) showing one reversible reduction wave (E^0 = 0.64 V) corresponding to the formation of (**2**; z = 0, L = CN). However, the electrochemistry of (**3**; z = 2, L = CNH) is more complex. Although the cyclic voltammogram, from 1.2 to 0.2 V, was poorly resolved it showed two reduction waves at *ca.* 0.66 and 0.93 V. The latter, larger wave is irreversible but may be assigned to the reduction of the dication (**3**; z = +2, L = CNH); it would be expected at a more positive potential than that for the reduction of the monocation (**3**; z = +1, L = CN). The second wave, at *ca.* 0.66 V, appears to be reversible and is very close in potential to that for the reduction of (**3**; z = +1, L = CN).

Although poor, these data suggest that (**3**; z = +2, L = CNH) is reduced to (**2**; z = +1, L = CNH) which then loses either a proton, to give (**2**; z = 0, L = CN), or a hydrogen atom, to give (**3**; z = +1, L = CN). No distinction can be made from the available electrochemical data. However, i.r. spectroscopic studies of the chemical reduction of (**3**; z = +2, L = CNH) with $[NBu^n_4][BH_4]$ show (**3**; z = +1, L = CN) as an intermediate, supporting the suggestion of hydrogen atom loss from (**2**; z = +1, L = CNH) before the final formation of (**2**; z = 0, L = CN).

All of the isolated examples of (**3**) display well resolved e.s.r. spectra at low temperature, confirming that the paramagnetic cations contain low-spin manganese(II) centres; the frozen solution (CH_2Cl_2–thf, 1:2; −110 °C) spectrum of (**3**; z = +1, L = CN) is shown in Figure 5. Apart from our own studies[9] on *trans*-$[MnL(CO)(dppm)_2]^z$ (z = +1, L = CN or NCS; z = +2, L = NCMe, CNMe, or $CNBu^t$), previous reports of the e.s.r. spectra of manganese(II) carbonylphosphines have noted only the presence of manganese hyperfine coupling.[3,8] Indeed, it has been stated that the absence of ^{31}P hyperfine coupling was indicative of little delocalisation of electron density onto the phosphine ligands, in contrast to isoelectronic molybdenum(I) complexes such as *trans*-$[Mo(CO)_2(dppm)_2]^+$.[3]

A preliminary analysis of the anisotropic spectrum of (**3**; z = +1, L = CN) clearly shows both manganese $[A(^{55}Mn), I = \frac{5}{2}]$ and phosphorus $[A(^{31}P), I = \frac{1}{2}]$ hyperfine coupling; one g component is split into a sextet (161 G), each line of which is further divided into a doublet of triplets by coupling to the $P(OPh)_3$ (43 G) and dppm (27 G) donor atoms.

A detailed analysis of the e.s.r. spectrum of (**3**; $z = +1$, L = CN) is in progress.[16] It is clear, however, that delocalisation of unpaired electron density onto the phosphorus atoms of (**3**) is likely to be similar to that in related chromium(I)[17] and molybdenum(I)[3] carbonylphosphines; poor spectral resolution rather than lack of delocalisation accounts for the previous absence of ^{31}P hyperfine coupling in the e.s.r. spectra of manganese(II) carbonylphosphines.[3,8]

Experimental

The preparation, purification, and reactions of the complexes were carried out in flasks shielded from light by aluminium foil, and under an atmosphere of dry nitrogen; i.r. spectroscopy was used to monitor the course of the reactions. Unless stated otherwise, products (*i*) were purified by dissolving in CH_2Cl_2, filtration, addition of n-hexane and partial evaporation of the solvent mixture *in vacuo* to induce precipitation, and (*ii*) dissolved in polar solvents such as CH_2Cl_2 or CH_3NO_2 to give air-sensitive solutions. The compounds *trans*-[MnL(CO)$_2${P(OPh)$_3$}(dppm)]^z ($z = 0$, L = Br or CN;[5] $z = +1$, L = CNMe[15]), *cis,cis*-[MnL(CO)$_2${P(OPh)$_3$}(dppm)]^z [$z = 0$, L = Br, NCS, or CN;[15] $z = +1$, L = py, NCMe,[5] CNMe,[15] or P(OPh)$_3$[5]], and N(C_6H_4Br-*p*)$_3$[18] were prepared by published methods. The salt [NO][PF$_6$] was purchased from Fluorochem Ltd., Glossop, Derbyshire.

Infrared spectra were recorded on a Nicolet MX-5 FT spectrometer, or a Perkin-Elmer PE 257 spectrometer with calibration against the absorption band of polystyrene at 1 601 cm^{-1}. *X*-Band e.s.r. spectra were recorded on a Varian Associates 4502/15 instrument and were calibrated against a 10^{-4} mol dm^{-3} aqueous solution of $K_2[NO(SO_3)_2]$ (5×10^{-2} mol dm^{-3} in K_2CO_3 as buffer) or a solid sample of the diphenylpicrylhydrazyl (dpph) radical. Electrochemical studies were carried out as described previously.[9] Solutions were 0.5×10^{-3} mol dm^{-3} and 1.0×10^{-3} mol dm^{-3} in complex for voltammetry and controlled potential electrolysis respectively; in both cases the solutions were 0.1 mol dm^{-3} in [NBu$^n_4$][PF$_6$] as supporting electrolyte. Under these conditions, E^0 for the couples $[Fe(\eta\text{-}C_5H_5)_2]^+$–$[Fe(\eta\text{-}C_5H_5)_2]$ and $[Fe(\eta\text{-}C_5Me_5)_2]^+$–$[Fe(\eta\text{-}C_5Me_5)_2]$ are 0.47 and −0.07 V respectively. Microanalyses were carried out by the staff of the Microanalytical Service of the School of Chemistry, University of Bristol.

trans-*[Bis(diphenylphosphino)methane]bromodicarbonyl(triphenyl phosphite)manganese(*II*) Hexafluorophosphate, trans*-[MnBr(CO)$_2${P(OPh)$_3$}(dppm)][PF$_6$].—Solid [NO][PF$_6$] (0.045 g, 0.26 mmol) was added to a stirred solution of *cis,cis*-[MnBr(CO)$_2${P(OPh)$_3$}(dppm)] (0.20 g, 0.22 mmol) in CH_2Cl_2 (25 cm^3). After 30 min the crimson solution was filtered and n-hexane (60 cm^3) added to precipitate the product. The solid was washed with toluene (2 × 30 cm^3) and then further purified from CH_2Cl_2–n-hexane to give crimson crystals, yield 0.16 g (72%).

The complex is soluble in polar solvents such as CH_2Cl_2, thf, and $MeNO_2$ to give deep red solutions which only slowly decompose in air; the solid may be stored for months at −20 °C under nitrogen.

trans-*[Bis(diphenylphosphino)methane]dicarbonylcyano(triphenyl phosphite)manganese(*II*) Hexafluorophosphate, trans*-[Mn(CN)(CO)$_2${P(OPh)$_3$}(dppm)][PF$_6$].—A deep blue solution of [N(C_6H_4Br-*p*)$_3$][PF$_6$], prepared by stirring N(C_6H_4Br-*p*)$_3$ (0.15 g, 0.24 mmol) in CH_2Cl_2 (25 cm^3) with [NO][PF$_6$] (0.04 g, 0.24 mmol) for 12 min while passing a rapid stream of nitrogen gas through the mixture, was filtered into a solution of *cis,cis*-[Mn(CN)(CO)$_2${P(OPh)$_3$}(dppm)] (0.20 g, 0.22 mmol) in CH_2Cl_2 (30 cm^3). After 10 min the solution was filtered, hexane (40 cm^3) added, and partial evaporation of the solvent *in vacuo* gave a crimson solid. Purification from CH_2Cl_2–n-hexane, followed by washing with toluene (2 × 30 cm^3) gave the product as air-sensitive crimson crystals, yield 0.16 g (69%).

trans-*[Bis(diphenylphosphino)methane]dicarbonyl(hydrogen isocyanide)(triphenyl phosphite)manganese Bis(hexafluorophosphate), trans*-[Mn(CNH)(CO)$_2${P(OPh)$_3$}(dppm)][PF$_6$]$_2$.—To a solution of *cis,cis*-[Mn(CN)(CO)$_2${P(OPh)$_3$}(dppm)] (0.18 g, 0.22 mol) in CH_2Cl_2 (20 cm^3) was added [NO][PF$_6$] (0.085 g, 0.49 mmol). After stirring for 45 min the purple solution was filtered, and n-hexane (60 cm^3) added to precipitate the product. Purification from CH_2Cl_2–n-hexane followed by washing with toluene (2 × 30 cm^3) gave purple crystals, yield 0.14 g (65%).

Crystal Structure Analysis of cis,cis-[MnBr(CO)$_2${P(OPh)$_3$}(dppm)] (**1**; $z = 0$, L = Br).—*Crystal data.* $C_{45}H_{37}BrMnO_5P_3$, $M = 885.5$, monoclinic, space group $C2/c$ (no. 15), $a = 14.827(5)$, $b = 19.526(5)$, $c = 28.367(8)$ Å, $\beta = 95.15(3)^0$, $U = 8\,179(5)$ Å^3, $T = 294$ K, $Z = 8$, $D_c = 1.45$ g cm^{-3}, $D_m = 1.41$ g cm^{-3}, $F(000) = 3\,616$, graphite monochromated Mo-K_α *X*-radiation, $\lambda = 0.710\,69$ Å.

Diffraction measurements were made on a single crystal of (**1**; $z = 0$, L = Br) (approximate dimensions 0.4 × 0.4 × 0.2 mm) mounted in a thin-walled glass capillary under N_2, at room temperature using a Nicolet *P*3*m* diffractometer. Intensity data were collected by Wyckoff ω-scans for a unique quadrant of reciprocal space in the range $4 < 2\theta < 50°$. Of 8 220 intensities measured, 7 211 remained after averaging of duplicate and symmetry equivalent measurements. Of these, 4 967 with $I > 1.5\sigma(I)$ were used in structure solution and refinement. An absorption correction was applied to these data, based on 400 azimuthal scan measurements; transmission coefficients varied between 0.418 and 0.595. The structure was solved by conventional heavy-atom methods and refined by blocked-cascade least squares. All non-hydrogen atoms were assigned anisotropic vibrational parameters; hydrogen atoms having isotropic parameters were constrained to idealised geometries (C–H 0.96 Å). Refinement converged to final residuals *R* 0.061, *R′* 0.059, and *S* 1.28,* where weights $w = [\sigma_c^2(F_o) + 0.0005F_o^2]^{-1}$ were assigned [$\sigma_c^2(F_o)$ being variance in F_o due to counting statistics]. Final electron-density difference maps showed no features of magnitude >0.62 e Å^{-3}. Complex neutral atom scattering factors were taken from ref. 19. All calculations were made using the SHELXTL program system.[20] Additional material available from the Cambridge Crystallographic Data Centre comprises thermal parameters, H-atom co-ordinates, and remaining bond lengths and angles.

Acknowledgements

We thank the S.E.R.C. for a research studentship (to S. J. R.), the British Council and Spanish Ministry of Education and Science for an Acciones Intergradas grant, and the Spanish Comision Asesora de Investigacion Cientifica y Tecnica (C.A.I.C.Y.T.) for support.

References

1 A. M. Bond, B. S. Grabaric, and Z. Grabaric, *Inorg. Chem.*, 1978, **17**, 1013.
2 A. M. Bond, R. Colton, and M. E. McDonald, *Inorg. Chem.*, 1978, **17**, 2842.

---

* $R = \Sigma||F_o| - |F_c||/\Sigma|F_o|$, $R' = [\Sigma w(|F_o| - |F_c|)^2/\Sigma w|F_o|^2]^{\frac{1}{2}}$, and $S = [\Sigma w(|F_o| - |F_c|)^2/(N_{obs} - N_{var})]^{\frac{1}{2}}$.

3 A. M. Bond, R. Colton, and M. J. McCormick, *Inorg. Chem.*, 1977, **16**, 155.

4 F. L. Wimmer, M. R. Snow, and A. M. Bond, *Inorg. Chem.*, 1974, **13**, 1617.

5 F. Bombin, G. A. Carriedo, J. A. Miguel, and V. Riera, *J. Chem. Soc., Dalton Trans.*, 1981, 2049.

6 R. H. Reimann and E. Singleton, *J. Chem. Soc., Dalton Trans.*, 1973, 841.

7 R. H. Reimann and E. Singleton, *J. Chem. Soc., Dalton Trans.*, 1973, 2658.

8 M. R. Snow and M. H. B. Stiddard, *J. Chem. Soc. A*, 1966, 777.

9 G. A. Carriedo, V. Riera, N. G. Connelly, and S. J. Raven, *J. Chem. Soc., Dalton Trans.*, 1987, 1769.

10 N. G. Connelly, S. J. Raven, G. A. Carriedo, and V. Riera, *J. Chem. Soc., Chem. Commun.*, 1986, 992.

11 F. J. Garcia Alonso, V. Riera, M. L. Valin, D. Moreiras, M. Vivanco, and X. Solans, *J. Organomet. Chem.*, 1987, **326**, C71.

12 G. A. Carriedo, N. G. Connelly, M. C. Crespo, I. C. Quarmby, and V. Riera, *J. Chem. Soc., Chem. Commun.*, 1987, 1806.

13 J. Chatt, C. T. Kan, G. J. Leigh, C. J. Pickett, and D. R. Stanley, *J. Chem. Soc., Dalton Trans.*, 1980, 2032.

14 A. M. Bond, R. Colton, and J. J. Jackowski, *Inorg. Chem.*, 1975, **14**, 274.

15 G. A. Carriedo, M. C. Crespo, V. Riera, M. G. Sanchez, M. L. Valin, D. Moreiras, and X. Solans, *J. Organomet. Chem.*, 1986, **302**, 47; G. A. Carriedo, M. C. Crespo, V. Riera, M. L. Valin, D. Moreiras, and X. Solans, *Inorg. Chim. Acta*, 1986, **121**, 191.

16 P. H. Rieger, unpublished work.

17 A. M. Bond, S. W. Carr, and R. Colton, *Inorg. Chem.*, 1984, **23**, 2343.

18 T. N. Baker, W. P. Doherty, jun., W. S. Kelley, W. Newmeyer, J. E. Rogers, jun., R. E. Spalding, and R. I. Walter, *J. Org. Chem.*, 1965, **30**, 3714.

19 'International Tables for *X*-Ray Crystallography,' Kynoch Press, Birmingham, 1974, vol. 4.

20 G. M. Sheldrick, SHELXTL, Revision 5.1, Göttingen, 1985.

Received 27*th July* 1987; *Paper* 7/1363